NeuroImage **14,** 617–631 (2001)
doi:10.1006/nimg.2001.0858, available online at http://www.idealibrary.com on IDEAL®

Human Somatosensory Area 2: Observer-Independent Cytoarchitectonic Mapping, Interindividual Variability, and Population Map

Christian Grefkes,*,†,[1] Stefan Geyer,‡ Thorsten Schormann,‡ Per Roland,§ and Karl Zilles*,†,‡

*C. and O. Vogt Brain Research Institute and ‡Department of Neuroanatomy, University of Düsseldorf, 40001 Düsseldorf, Germany; †Institute of Medicine, Research Center Jülich, 52425 Jülich, Germany; and §Division of Human Brain Research, Karolinska Institute, 17177 Stockholm, Sweden

Received November 30, 2000

We analyzed the topographical variability of human somatosensory area 2 in 10 postmortem brains. The brains were serially sectioned at 20 μm, and sections were stained for cell bodies. Area 2 was delineated with an observer-independent technique based on significant differences in the laminar densities of cell bodies. The sections were corrected with an MR scan of the same brain obtained before histological processing. Each brain's histological volume and representation of area 2 was subsequently reconstructed in 3-D. We found that the borders of area 2 are topographically variable. The rostral border lies between the convexity of the postcentral gyrus and some millimeters deep in the rostral wall of the postcentral sulcus. The caudal border lies between the fundus of the postcentral sulcus and some millimeters above it in the rostral wall. In contrast to Brodmann's map, area 2 does not extend onto the mesial cortical surface or into the intraparietal sulcus. When the postcentral sulcus is interrupted by a gyral bridge, area 2 crosses this bridge and is not separated into two segments. After cytoarchitectonic analysis, the histological volumes were warped to the reference brain of a computerized atlas and superimposed. A population map was generated in 3-D space, which describes how many brains have a representation of area 2 in a particular voxel. This microstructurally defined population map can be used to demonstrate activations of area 2 in functional imaging studies and therefore help to further understand the role of area 2 in somatosensory processing.

Key Words: **postcentral gyrus; parietal cortex; 3-D reconstruction; morphometry; brain atlas.**

INTRODUCTION

Both in monkeys and in humans the classical primary somatosensory cortex consists of four different areas (Brodmann, 1909; Vogt and Vogt, 1919; von Economo and Koskinas, 1925; Powell and Mountcastle, 1959a), which differ in cytoarchitecture and process different submodalities of the somatosensory system. Area 3a in the depth of the central sulcus receives its input mainly from muscle spindles. Area 3b in the rostral wall of the postcentral gyrus receives afferents from both rapidly and slowly adapting cutaneous receptors, area 1 on the vertex of the postcentral gyrus predominantly from rapidly adapting cutaneous receptors. Caudal to area 1 lies area 2 which receives input mainly from deep receptors in joints (Kaas, 1993, 1997). The electrophysiological properties of these areas have been extensively characterized in monkeys. In contrast to areas 3b and 1, neurons in area 2 respond to more complex cutaneous stimuli (e.g., direction or orientation of a stimulus) or to active tactile discrimination tasks (Hyvärinen and Poranen, 1978; Gardner and Costanzo, 1980; Costanzo and Gardner, 1980; Iwamura *et al.*, 1983a, 1983b; Warren *et al.*, 1986; Ruiz *et al.*, 1995). Much of this knowledge has been gained from studies in nonhuman primates in which direct comparisons between structure and function are fairly easy to perform since upon completion of the electrophysiological part of the study the brains can be sectioned, sections can be stained for cell bodies, and penetration sites can be directly correlated with the cytoarchitectonic pattern. For obvious ethical reasons, such an approach is not feasible in humans.

Many cytoarchitectonic maps of the human cortex have been published in the first half of the 20th Century (Campbell, 1905; Brodmann, 1909; von Economo and Koskinas, 1925; Bailey and von Bonin, 1951; Sarkissov *et al.*, 1955). These "classical" brain maps, however, were published in a 2-dimensional print format. They are schematic drawings which reflect the topographical situation in one representative brain (usually only on its exposed cortical surface since the sulci are not opened up). The problem of interindividual macro- (see, e.g., Ono *et al.*, 1990) and microan-

1053-8119/01 $35.00

atomical (see, e.g., Rademacher *et al.*, 1993) variability is not taken into consideration. Furthermore, "classical" brain maps are "rigid", i.e., they are not based on a spatial reference system and cannot be adapted to individual brains. Hence, multimodal integration of structural and functional data obtained from different brains is impossible.

A second problem is the subjectivity underlying any cytoarchitectonic parcellation of the cortex. In the past, it had not been possible to define borders between cortical areas in an objective and observer-independent way. Biological variability *and* each investigator's subjective criteria have influenced the results and introduced considerable variations. These two factors (which cannot be disentangled) have led to the well-known differences between the maps published by different authors.

To overcome many of these problems, a new approach has recently been introduced: Cortical areas are delineated with an observer-independent cytoarchitectonic technique in postmortem brains (Schleicher *et al.*, 1999) and are then transferred to a computerized brain atlas (Roland and Zilles, 1994). For each area, a volume of interest (VOI) can then be defined which is not based on macroanatomical landmarks of the cortex but instead on cytoarchitectonic mapping of postmortem brains. Somatosensory areas 3a, 3b, and 1 have already been mapped with this technique (Geyer *et al.*, 1999, 2000). In a functional study (Bodegard *et al.*, 2000), regional cerebral blood flow changes were determined with PET when subjects discriminated differences in the speed of a moving stimulus. The PET data were transferred to the computerized atlas and superimposed with the microstructural VOIs of areas 3a, 3b, and 1. The activation cluster significantly overlapped with areas 3b and 1 but, in addition, extended further caudally into the cortex along the postcentral sulcus. Could this mean that area 2 was also activated by this task? Electrophysiological studies in monkeys have shown that a mechanical stimulus with a fixed orientation in space is an adequate stimulus for neurons in area 2. However, in functional imaging studies in humans, an activation of area 2 can be postulated but it cannot be proven since borders between cortical areas are not visible even on high-resolution MR scans and they are topographically variable across different individuals (Rademacher *et al.*, 1993; Roland and Zilles, 1994; Rajkowska and Goldman-Rakic, 1995; Geyer *et al.*, 1996, 1999; Roland and Zilles, 1996; White *et al.*, 1997; Roland *et al.*, 1997; Amunts *et al.*, 1999; Amunts *et al.*, 2000).

As a further step toward a solution of this problem, the present study was performed. We mapped somatosensory area 2 in an observer-independent way in 10 postmortem brains. The 10 volume representations were then warped to the reference brain of the computerized atlas, superimposed in 3-D space, and a microstructural population map of area 2 was generated. Superimposition with PET or fMRI data in the same reference space should then give a more valid answer to the question whether or not area 2 is being activated by a somatosensory task.

MATERIALS AND METHODS

The main steps are summarized as a flowchart in Table 1.

Histological and MR Processing of the Brains

The analysis was done in 10 postmortem human brains (5 males, 5 females) obtained at autopsy from subjects with no known history of neurological or psychiatric diseases (age range 37–85 years, mean age 68.9 years, cf. Table 2). All subjects had given written consent before death and/or had been included in the body donor program of the Department of Anatomy, University of Düsseldorf, Germany. The brains were removed from the skull and fixed in 4% formaldehyde or in Bodian's fixative (90 ml of 80% ethanol, 5 ml of 37% formaldehyde, 5 ml of glacial acetic acid) for approximately 5 months. Fixation was done in a freely floating way, i.e., by suspending the brains at the basilar artery to avoid compression or distortions. After fixation, T1 weighted MR scans (1.5 T Siemens Magnetron SP scanner, 3-D fast low angle shot (3-D FLASH) pulse sequence, flip angle = 40°, TR = 40 ms, TE = 5 ms, voxel size = 1.17 mm (mediolateral) × 1 mm (rostrocaudal) × 1 mm (dorsoventral)) were acquired for documentation of brain size and shape before subsequent histological processing, which leads to shrinkage and distortions of the brains. The brains were dehydrated in graded alcohols, embedded in paraffin, and serially sectioned (20 μm whole brain sections) in a coronal (9 brains) or sagittal (1 brain) plane with a microtome for large sections. Images of the paraffin blockface were obtained after each 60th section (coronal plane) or 45th section (sagittal plane) with a CCD camera (XC-75, Sony/Japan, image matrix 256 × 256 pixels, 8-bit gray value resolution). Each 60th section (coronal plane) or 45th section (sagittal plane) was mounted on a gelatin-coated slide and was stained for cell bodies with a Nissl-like method (Merker, 1983), which yields high contrast between cell bodies (black) and neuropil (light brown), a prerequisite for quantitative cytoarchitectonic analysis.

Observer-Independent Delineation of Cytoarchitectonic Borders

Rectangular regions of interest (ROIs) covering the postcentral gyrus and sulcus were defined in each cell-stained section in both hemispheres. Each ROI was scanned in a mosaic-like sequence with a CCD camera (XC-75, Sony/Japan, image matrix 512 × 512 pixel,

TABLE 1

Histological Processing and Cytoarchitectonic Analysis, 3-D Reconstruction of the Histological Volume, and Spatial Normalization

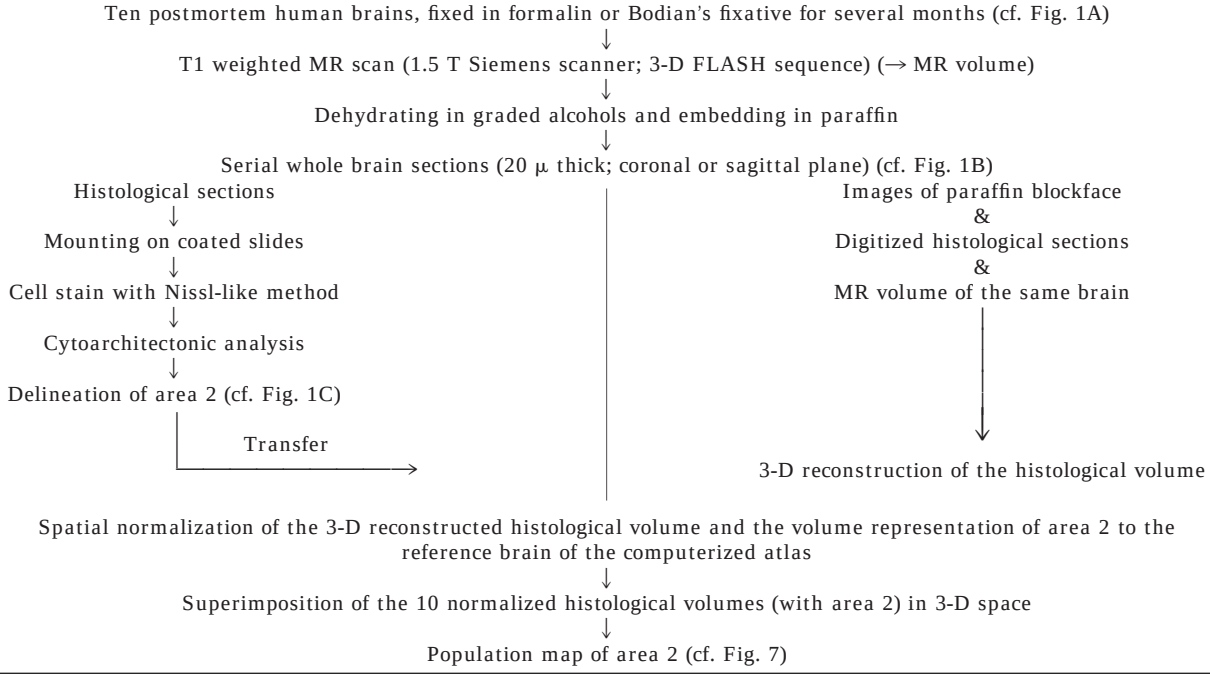

8-bit gray value resolution) attached to a microscope (Universal microscope, Zeiss/Germany, image size 540 × 540 μm), which was equipped with a computer-controlled motorized stage and an autofocus unit. The image sequence was further processed with an image analysis software package (KS 400, Version 3.0, Zeiss/Germany) and a standard PC. In each image (size 540 × 540 μm), the areal fraction of darkly stained cell bodies (gray level index; GLI) was measured after adaptive thresholding (Schleicher and Zilles, 1990) in square, adjoining fields (size 20 × 20 μm). This procedure was performed in each image of the sequence. The resulting data matrix covering the entire ROI is the GLI image (Schleicher and Zilles, 1990).

TABLE 2

Brains Used for the Delineation of Area 2

Brain	Sex	Age (years)	Cause of death	Fixative
207/84	Male	75	Toxic glomerulonephritis	Formalin
544/91	Female	79	Carcinoma of the bladder	Bodian
281/93	Male	68	Vascular disease	Formalin
189/92	Male	55	Carcinoma of the rectum	Formalin
68/95	Female	79	Cardiorespiratory insufficiency	Bodian
2/95	Female	85	Mesenteric artery infarction	Bodian
56/94	Female	72	Renal failure	Formalin
340/83	Female	79	Cardiorespiratory insufficiency	Formalin
146/86	Male	37	Right heart failure	Formalin
16/96	Male	54	Myocardial infarction	Formalin

Equidistant density profiles (125 μm wide, spacing between adjacent profiles 200 μm) covering the entire ROI were extracted from the GLI images perpendicularly to the cortical layers. The profiles extended from the border between layers I and II (outer contour) to the border between layer VI and the white matter (inner contour). Both contour lines were defined interactively in each GLI image with a graphics tablet, and equidistant profiles were automatically extracted from the GLI image (Schleicher *et al.*, 2000).

The profiles were standardized to a length of 101 points by resampling the data with linear interpolation in order to compensate for variations in cortical thickness. To quantify each profile's shape, 10 features based on the GLI distribution pattern across the cortical layers were calculated and combined into one feature vector. A mean feature vector was calculated from a block of b (e.g., $b = 12$) adjacent profiles, and another mean feature vector from a neighboring block of b adjacent profiles. Differences between the mean feature vectors from two neighboring blocks of profiles were calculated as Mahalanobis distances D^2 (Mahalanobis *et al.*, 1949). D^2 values were plotted as a function of the positions of the profile blocks within the ROI. The resulting distance function revealed maxima at those locations where the regions covered by profiles

showed differences in their laminar patterns. Statistical significance was evaluated by a Hotelling's T^2 test. The corresponding P values were Bonferroni-corrected for multiple comparisons. For each ROI, distance functions were calculated for blocksizes from $b = 8$ to $b = 20$, and the positions of significant maxima were plotted as a function of b (cf. Figs. 2 and 5). The positions of these maxima were then compared with the cytoarchitectonic pattern in the cell-stained sections. For further details see (Schleicher *et al.*, 1999, 2000; Geyer *et al.*, 1999).

In order to visualize the laminar neuronal pattern of area 1 and 2, 10 adjacent GLI profiles of each area were extracted from one representative section (right hemisphere of each brain). The sections were selected according to the following criteria: (i) No artifacts caused by histological processing, (ii) orientation of the sectioning plane perpendicular to the cortical surface, (iii) random selection of the sections fulfilling criteria (i) and (ii). The profiles were standardized in length and averaged, resulting in one mean profile for each area and brain. In a second step, the 10 mean profiles (each representing one brain) of each area were averaged again and plotted (cf. Figs. 4A and 4B). Profiles were not extracted from the posterior parietal cortex (PPC) caudal to area 2 since the PPC is cytoarchitectonically heterogeneous and the topography of its areas has not yet been elucidated in sufficient detail.

3-D Reconstruction of the Histological Volume

Each mounted and cell-stained histological section was digitized with the CCD camera (image matrix 256 × 256 pixels, 8-bit gray value resolution). The histological volume of the brain was then reconstructed in 3-D from the images of the paraffin blockface, the digitized histological sections, and the MR volume of the same brain using linear and nonlinear transformations (Schormann *et al.*, 1993, 1995, 1996, 1997a; Schormann and Zilles, 1997). Since the MR volume was obtained prior to histological processing, any artifacts (e.g., shrinkage of the brain due to dehydration in graded alcohols or compression of the sections due to cutting) could be eliminated in the 3-D reconstructed histological volume by matching it with the MR volume of the same brain. The statistically significant borders of area 2 were marked on the histological sections. With an image analysis software package and an interactive voxel-painting tool (KS 400, Version 3.0, Zeiss/Germany) the extent of area 2 was labeled in the corresponding sections of the reconstructed volume. Thus, a microstructurally defined representation of cytoarchitectonic area 2 was obtained in the 3-D reconstructed histological volume of each brain.

Area 2 is mostly hidden in the depth of the postcentral sulcus. Therefore, in order to reveal its topography in relation to the macroanatomy of the postcentral gyrus, the gray matter of the reconstructed histological volume was interactively segmented from the underlying white matter with the KS 400 software package. The extent of area 2 was then traced along the gray/white matter interface (cf. Figs. 6A and 6B). The volume was filtered with an isotropic Gaussian kernel (FWHM = 1 mm) and the surface of the gray/white matter interface (with the extent of area 2) was rendered in 3-D with the AVS Express software (AVS Inc., Waltham, MA) (cf. Figs. 6C and 6D).

Spatial Normalization

Each 3-D reconstructed histological volume (with the volume representation of area 2; prior to gray/white matter segmentation) was spatially normalized to the reference brain of the computerized atlas (which is oriented in the Talairach coordinate system; see Roland *et al.*, 1994) with a new algorithm based on an extended principal axes theory (Schormann *et al.*, 1997b) and a fast automated multiresolution full-multigrid movement model (Schormann and Zilles, 1997, 1998; Schormann, 1998).

The 10 normalized histological volumes (with the representations of area 2) were superimposed in the 3-D space of the reference brain and a population map was generated for area 2, which describes, for each voxel, how many brains have a representation of area 2 in this particular voxel. For further details see Geyer *et al.* (2000).

RESULTS

Observer-Independent Cytoarchitectonic Mapping of Area 2

Figure 1A shows a dorsal view of brain 340/83 after fixation in formalin for 5 months. Sagittal whole brain section no. 3811 (cf. dashed line in Fig. 1A) is depicted in Fig. 1B. The box in Fig. 1B marks the ROI encompassing the postcentral gyrus and postcentral sulcus which was used for calculation of the GLI and subsequent extraction of profiles. The corresponding GLI image of the ROI is shown at a higher magnification in Fig. 1C. Equidistant profiles 200 μm apart were extracted from the crown of the postcentral gyrus (index 1) to the fundus of the postcentral sulcus (index 97). In Fig. 1D, the D^2 values of the Mahalanobis distance function ($b = 14$) are plotted against the indices which indicate the positions of the profiles in the cortex. Two significant maxima are marked with drop lines ($P < 0.001$; after Bonferroni correction).

In Fig. 2B, the effect of increasing values of b (i.e., numbers of adjacent profiles per block) is demonstrated by processing the same set of profiles as shown in Fig. 1C for $b = 8$ to $b = 20$. Only the positions of significant maxima and their levels of significance are indicated

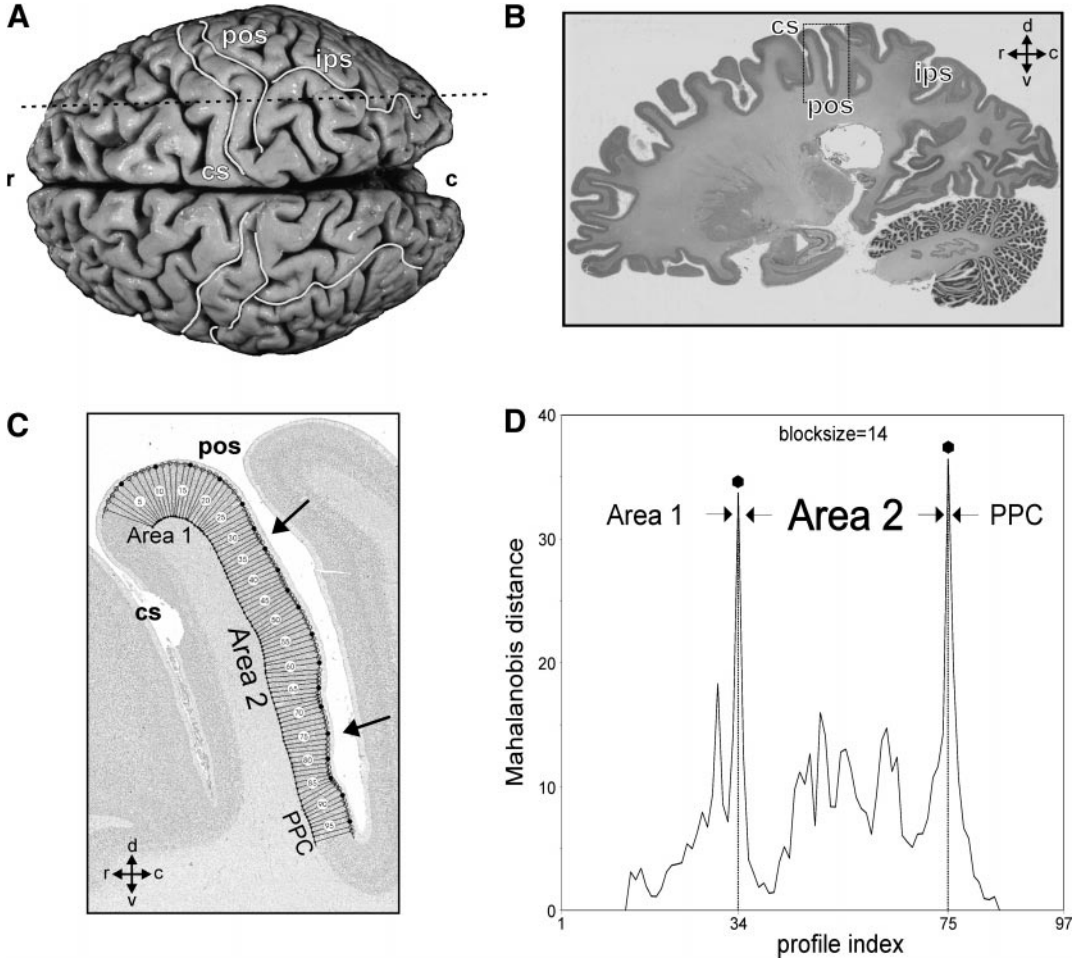

FIG. 1. (A) Dorsal view of postmortem brain 340/83 after fixation for 5 months in formalin. The postcentral sulcus (pos) is connected with the intraparietal sulcus (ips) in both hemispheres. (B) Sagittal section 3811 through A (cf. dashed line in A). Box shows region of interest (ROI) encompassing the cortex along the postcentral sulcus (pos), which was used for gray level index (GLI) measurements and subsequent extraction of profiles. (C) GLI image (inverted before printing) of the ROI (cf. B) at a higher magnification. Equidistant profiles 200 μm apart were extracted from index 1 on the crown of the postcentral gyrus to index 97 close to the fundus of the postcentral sulcus (pos). (D) Mahalanobis distance function (ordinate) plotted against the indices of these profiles (cf. C). Two significant maxima are marked with drop lines. Symbols indicate level of significance ($P < 0.001$). The positions of these two maxima are marked with arrows in C. cs, central sulcus; PPC, posterior parietal cortex; r, rostral; c, caudal; d, dorsal; v, ventral.

(dotted horizontal line at $b = 14$ corresponds to plot shown in Fig. 1D). The degree of smoothing increases with a higher number of profiles per block but the positions of two significant maxima are remarkably stable. Across a wide range of b, the maxima indicating the borders between area 1 and area 2 and between area 2 and the PPC can be found at similar positions in the cortex (cf. schematic drawing in Fig. 2B, approximate Talairach plane x = +29 mm).

The positions of these significant maxima can be reproduced at comparable positions across a sequence of sagittal sections (distance between adjacent sections 0.9 mm) from the same brain (340/83) (Figs. 2A–2D). The maximum at index 31 in section 3766 (Fig. 2A, $x = +28$ mm) lies close to the caudal shoulder of the postcentral gyrus and corresponds to the maxima at index 32 in section 3811 (Fig. 2B, $x = +29$ mm), 19 in section 3856 (Fig. 2C, $x = +30$ mm), and 19 in section 3901 (Fig. 2D, $x = +31$ mm) (cf. schematic drawings). The maximum at index 62 in section 3766 (Fig. 2A) lies further down in the depth of the postcentral sulcus and corresponds to the maxima at index 75 in section 3811 (Fig. 2B), 72 in section 3856 (Fig. 2C), and 82 in section 3901 (Fig. 2D).

The positions of the two significant maxima in the caudal bank of the postcentral gyrus coincide with visible changes in cytoarchitecture in the cell-stained sections. In section 3811 (brain 340/83, cf. Fig. 2B), the first change in cytoarchitecture is evident close to the caudal shoulder of the postcentral gyrus. At this position, granular cortex with a columnar arrangement of the cells, a band of large and elongated pyramidal cells in lower layer III, and a blurred border between layer VI and the underlying white matter merges into gran-

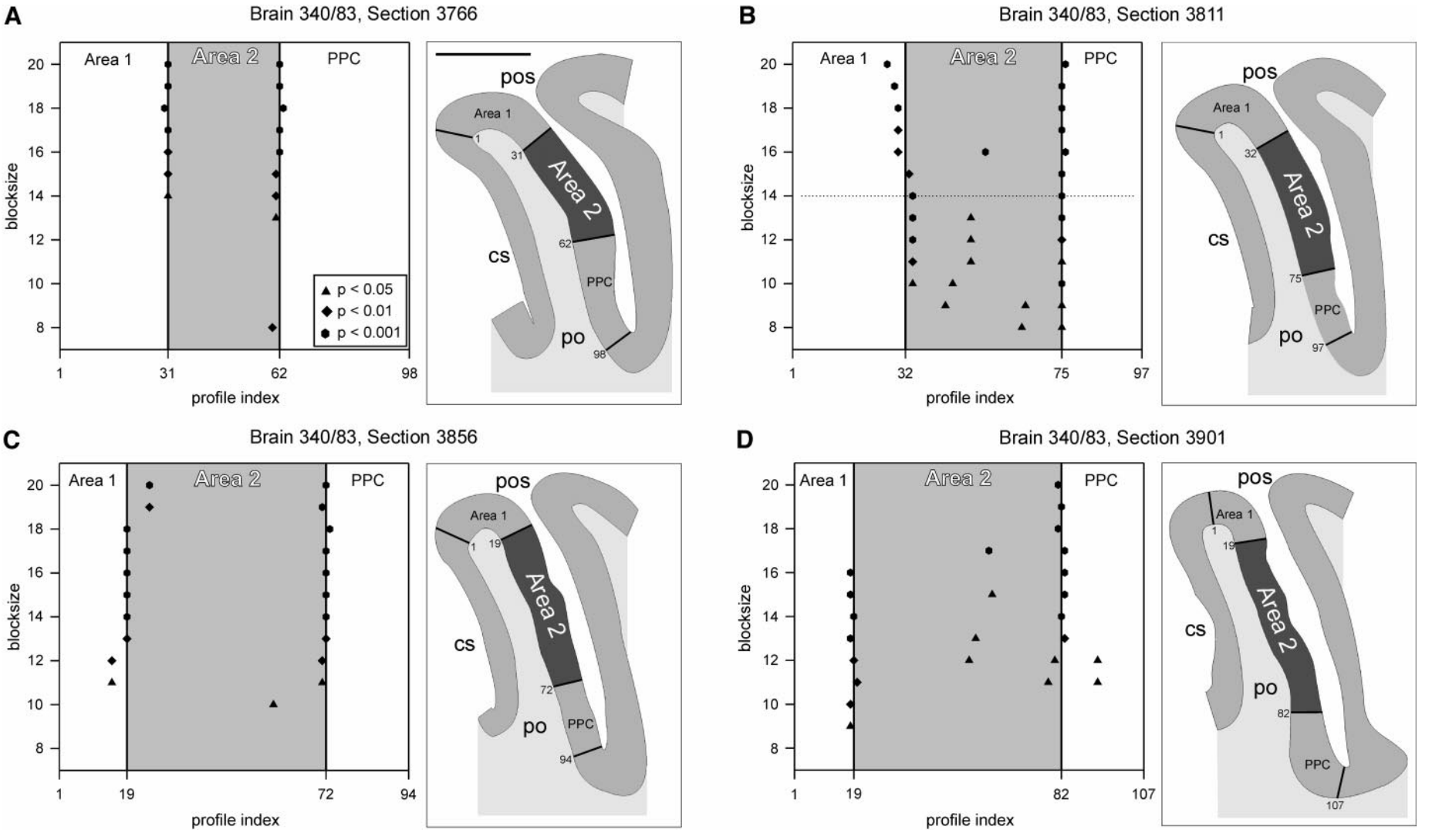

FIG. 2. Positions of maxima in the caudal wall of the postcentral gyrus (po; abscissa) and their levels of significance plotted against blocksize (ordinate) across a mediolateral sequence of sagittal sections (distance between adjacent sections 0.9 mm) from the same brain (340/83): sections 3766 (corresponding to the approximate Talairach plane x = +28 mm; A), 3811 (x = +29 mm; B), 3856 (x = +30 mm; C), and 3901 (x = +31mm; D). Dotted horizontal line in B corresponds to plot in Fig. 1D. Extent of area 1, area 2 (dark gray), and the PPC is marked in the plots and the corresponding schematic drawings. For other conventions see Fig. 1. Bar, 5 mm (A–D).

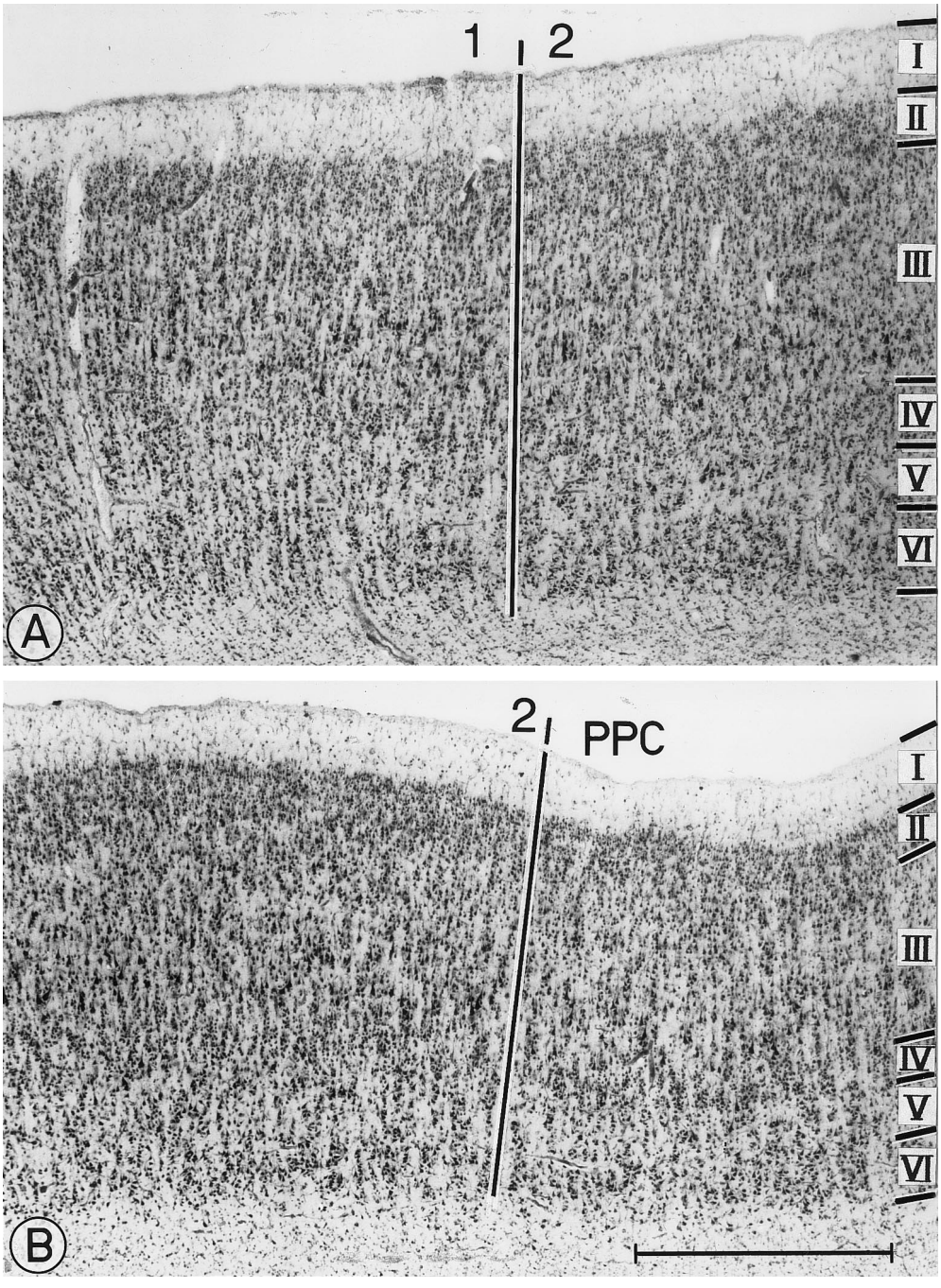

FIG. 3. Transitions between area 1 and 2 (A) and between area 2 and the PPC (B) in the caudal wall of the postcentral gyrus (brain 340/83, section 3811; cf. Figs. 1B–1D and 2B). Area 2 is characterized by a granular cortex with slightly lower cell density than in area 1, a less pronounced columnar arrangement of cells, smaller pyramids in layer III, and a sharp border between layer VI and the white matter. Roman numerals indicate cortical layers. Bar, 1 mm (A, B).

ular cortex with slightly lower cell density, a less pronounced columnar arrangement of the cells, smaller pyramids in layer III, and a sharp border between layer VI and the white matter (Fig. 3A). This transition corresponds to the border between somatosensory areas 1 and 2. It coincides with index 32 in section 3811 (cf. Fig. 2B) and the corresponding maxima in the other sections of the sequence (cf. Figs. 2A–2D). The second change in cytoarchitecture is evident further down in the depth of the postcentral sulcus. Across this border, the mean cell density decreases further, the columnar arrangement of the cells becomes more pronounced again, and the pyramids in lower layer III decrease even further in size (Fig. 3B). This transition corre-

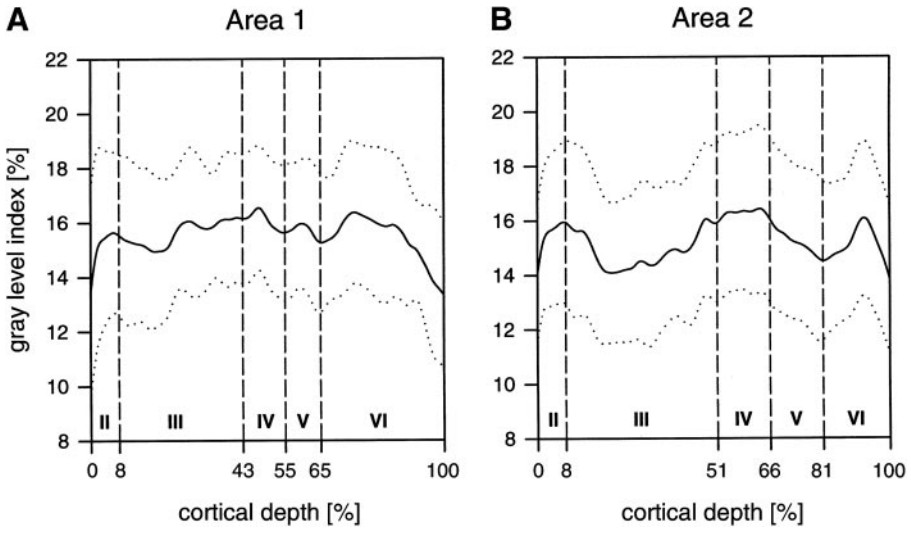

FIG. 4. Mean cell density profiles across layers II through VI (sampled from 10 right hemispheres) of area 1 (A) and area 2 (B). Mean gray level index (solid line) ± standard deviation (dotted lines) is plotted against cortical depth (roman numerals and dashed vertical lines indicate cortical layers).

sponds to the border between area 2 and the PPC. It coincides with index 75 in section 3811 (cf. Fig. 2B) and the corresponding maxima in the other sections of the sequence (cf. Figs. 2A–2D).

Mean density profiles (GLI against cortical depth) of areas 1 and 2 reflect the mean laminar pattern of the volume density of neurons across layers II through VI (Fig. 4). In area 2 (Fig. 4B), the mean volume density of neurons in the middle part of layer III is lower compared to area 1 (Fig. 4A), the density of layer VI neurons decreases more steeply towards the white matter (reflecting the sharper border between gray and white matter in area 2), and the infragranular layers (especially layer VI) are narrower in area 2 compared to area 1.

Interindividual Variability of Area 2

Figure 5 shows the topographical variability of area 2 across four different brains (sectioned in a coronal plane). One section per brain from a comparable rostrocaudal level (approximate Talairach plane $y = -29$ mm) is depicted schematically in Figs. 5A–5D. Area 2 always occupies the caudal wall of the postcentral gyrus. However, the positions of significant maxima of the Mahalanobis distance function and corresponding changes in cytoarchitecture in the cell-stained sections which represent the rostral border of area 2 (toward area 1) and its caudal border (towards the PPC) are topographically variable across different brains. The rostral border of area 2 may lie within the postcentral sulcus close to the caudal shoulder of the postcentral gyrus (Figs. 5A, 5B, and 5D) or it may lie on the exposed cortical surface towards the crown of the postcentral gyrus (Fig. 5C). Likewise, the caudal border of area 2 may lie close to the fundus of the postcentral sulcus (Figs. 5A and 5D) or it may lie somewhat away from it in the ascending part of the postcentral gyrus (Figs. 5B and 5C). There are no macroanatomical landmarks, which reliably indicate the positions of the rostral and caudal border of area 2. A similar degree of interindividual variability is also obvious on a macroanatomical level (Tables 3A and 3B). In maps of the human cerebral cortex, the postcentral sulcus is typically depicted as a continuous and uninterrupted structure. In our sample of 10 brains, however, this is the case only in 70% on the right and 40% on the left side. Two segments of the postcentral sulcus (with a gyral bridge in between) are observed in 20% (right) and 40% (left), three segments in 10% (right) and 20% (left). In 20% (right) and 40% (left), the postcentral sulcus reaches to the mesial surface. In 40% (right) and 30% (left), it is connected with the Sylvian fissure. The postcentral and intraparietal sulcus are connected in 90% (right and left). The intraparietal sulcus is continuous in 50% (right) and 70% (left), two segments are observed in 40% (right) and 30% (left), three segments in 10% (right) and 0% (left).

This variability in macroanatomy has little influence on the topography of area 2. Area 2 always occupies the caudal wall of the postcentral gyrus on the dorsolateral convexity of the brain. In those cases in which the intraparietal sulcus is connected with the postcentral sulcus (90% in the right and left hemisphere), area 2 does not extend into the intraparietal sulcus (Fig. 6D). The medial end of area 2 may reach to the midline or there may be a gap of up to several millimeters between its medial end and the midline irrespective of whether or not the postcentral sulcus reaches to the mesial cortical surface. We never observed area 2 to lie on the mesial surface (Fig. 6D). Likewise, the lateral

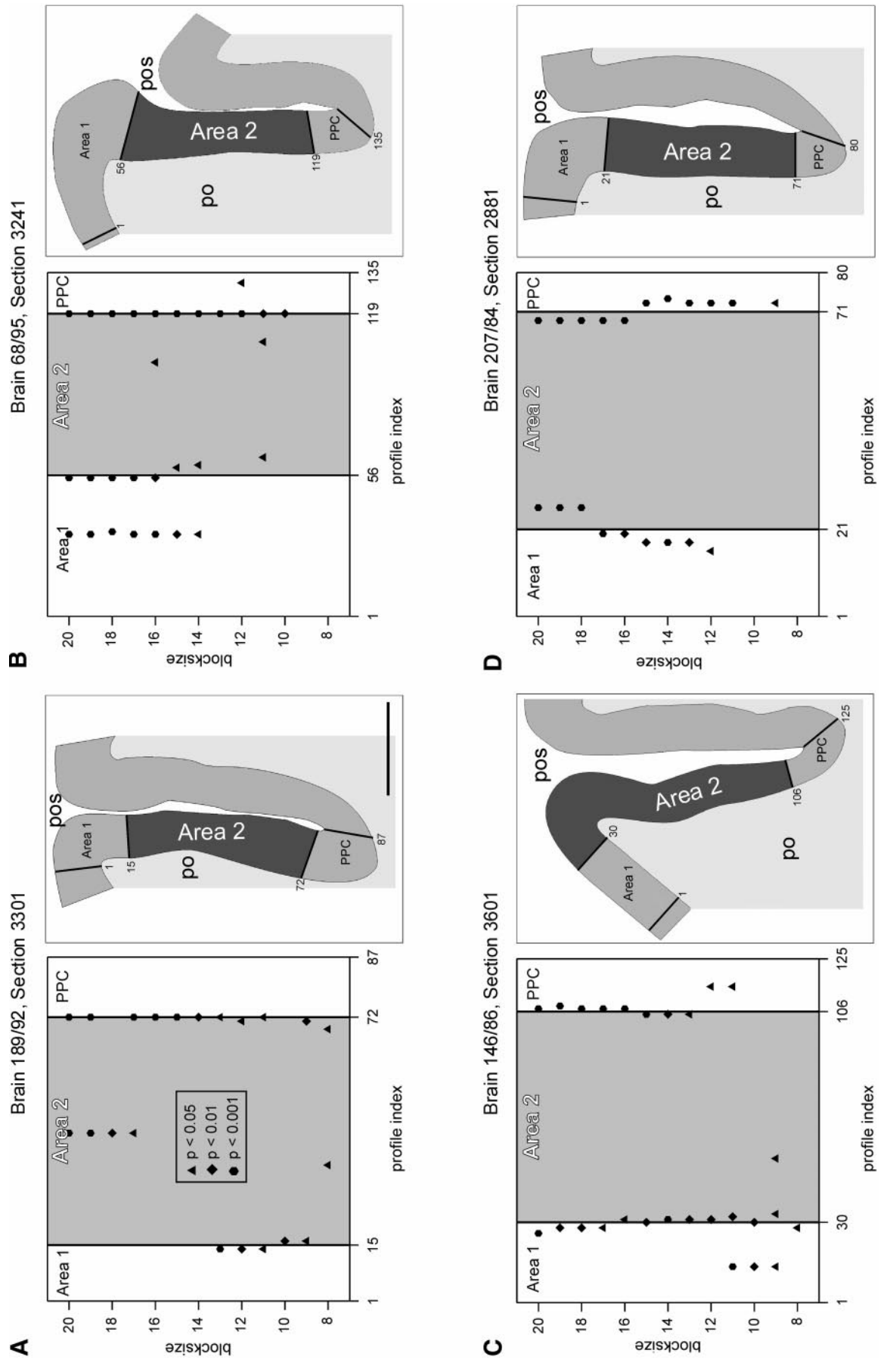

FIG. 5. Positions of maxima in the caudal wall of the postcentral gyrus (po; abscissa) and their levels of significance plotted against blocksize (ordinate) in four different brains (one coronal section per brain): brain 189/92, section 3301 (A), brain 68/95, section 3241 (B), brain 146/86, section 3601 (C), and brain 207/84, section 2881 (D). Sections correspond to the approximate Talairach plane $y = -29$ mm. Extent of area 1, area 2 (dark gray), and the PPC is marked in the plots and the corresponding schematic drawings. For other conventions see Figs. 1 and 2. Bar, 5 mm (A–D).

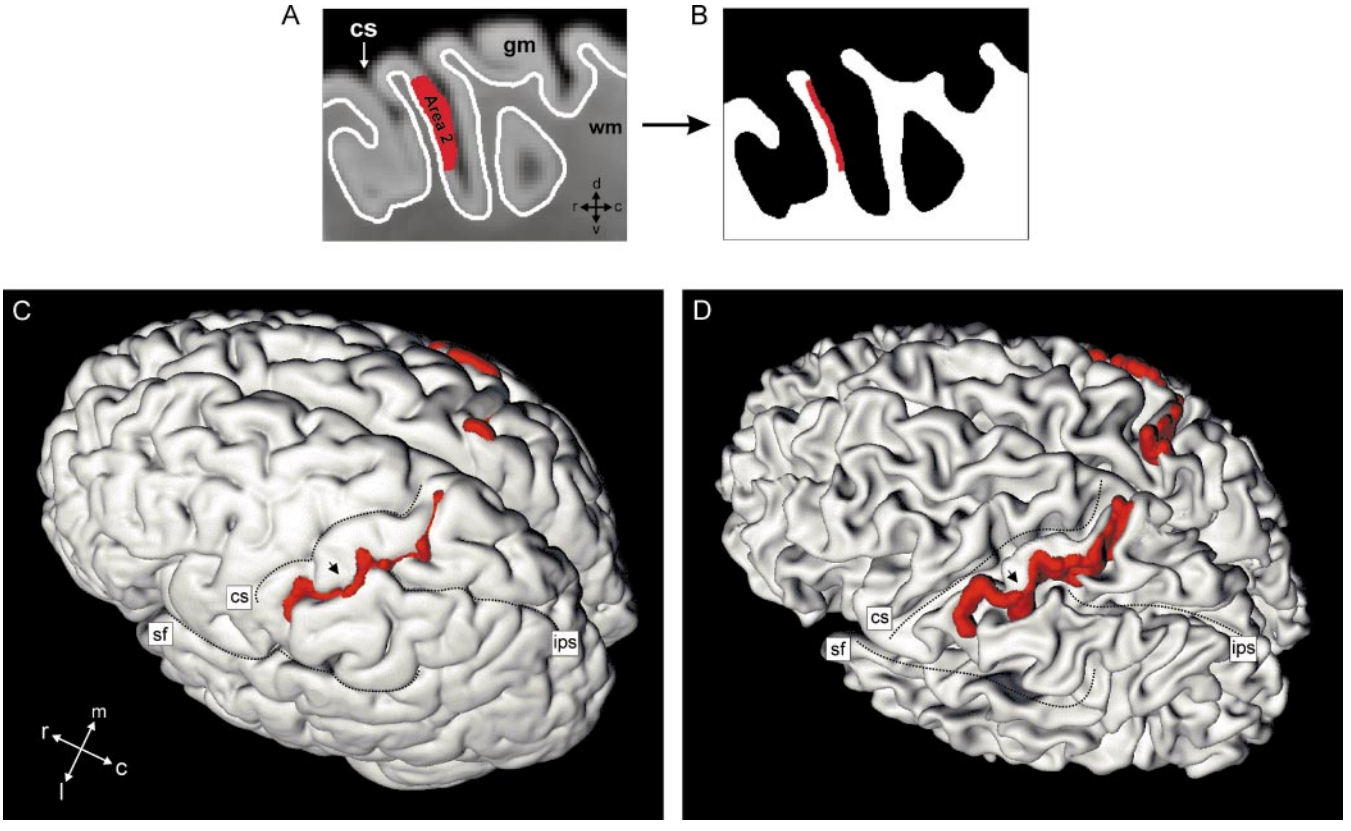

FIG. 6. 3-D reconstruction of the histological volume of brain 340/83 with extent of area 2. (A) Detail view of a sagittal section through the reconstructed histological volume (gray values have been inverted). Gray matter (gm)/white matter (wm) interface is marked in white. Area 2 is marked in red, as defined by observer-independent delineation in the corresponding cell-stained section (cf. Figs. 1B and 1C). (B) Same section as in A after segmentation of the gray matter from the underlying white matter. Area 2 is traced in red along the gray/white matter interface. (C) 3-D reconstruction of the pial surface of the histological volume (cf. A). Area 2 in the caudal wall of the postcentral gyrus is shown in red. Arrow indicates a cortical bridge which separates the postcentral sulcus into two segments. Left-dorsolateral point of view. (D) 3-D reconstruction of the gray/white matter interface of the histological volume (cf. B). Area 2 is shown in red. Arrow indicates the same cortical bridge as shown in C. Identical point of view as in C. cs, central sulcus; ips, intraparietal sulcus; sf, Sylvian fissure; r, rostral; c, caudal; d, dorsal; v, ventral; m, medial; l, lateral.

end of area 2 may reach to the Sylvian fissure or there may be a gap of up to several millimeters between its lateral end and the fissure irrespective of whether or not the postcentral sulcus is connected with the Sylvian fissure. We never observed area 2 to reach into the depth of the Sylvian fissure (Fig. 6D). In 30% (right) and 60% (left), the course of the postcentral sulcus is interrupted by gyral bridges (Table 3A). This situation, however, does not interrupt the course of area 2. As can be seen in Figs. 6C and 6D, area 2 crosses this bridge (marked by an arrow) and is not separated into two segments (a photograph of this brain is depicted in Fig. 1A).

Spatial Normalization and Population Map of Area 2

Each 3-D reconstructed histological volume (with the volume representation of area 2) was then spatially normalized to the reference brain of the computerized atlas. The 10 normalized volumes were superimposed in the 3-D space of the reference brain and a population map was generated for area 2 (Fig. 7; reference brain is shown in the background). The population map describes, for each voxel, how many brains have a representation of area 2 in this particular voxel. This representation is color coded in a spectral sequence from dark blue (area 2 is present in only 1 of 10 brains in this voxel) to dark red (in all 10 brains). Left-right differences in the topographical relationship between the central sulcus and the population map of area 2 are due to left-right differences in the macroanatomy of our reference brain. This brain is the *in vivo* MR scan of one normal human brain (cf. Roland *et al.*, 1994) and *not* a mean brain, cf. MNI-template. The entire volume of the population map (i.e., representation of area 2 in $\geq$1 of 10 brains) is: 20,018 mm^3 (left), 18,311 mm^3 (right), and 38,329 mm^3 (left + right). The Talairach coordinates of the bounding box of the map's entire volume are for the left hemisphere: $x_{medial} = -6$ mm, $x_{lateral} = -62$ mm, $y_{rostral} = 0$ mm, $y_{caudal} = -59$ mm, $z_{dorsal} = +69$ mm, $z_{ventral} = +22$ mm. For the right

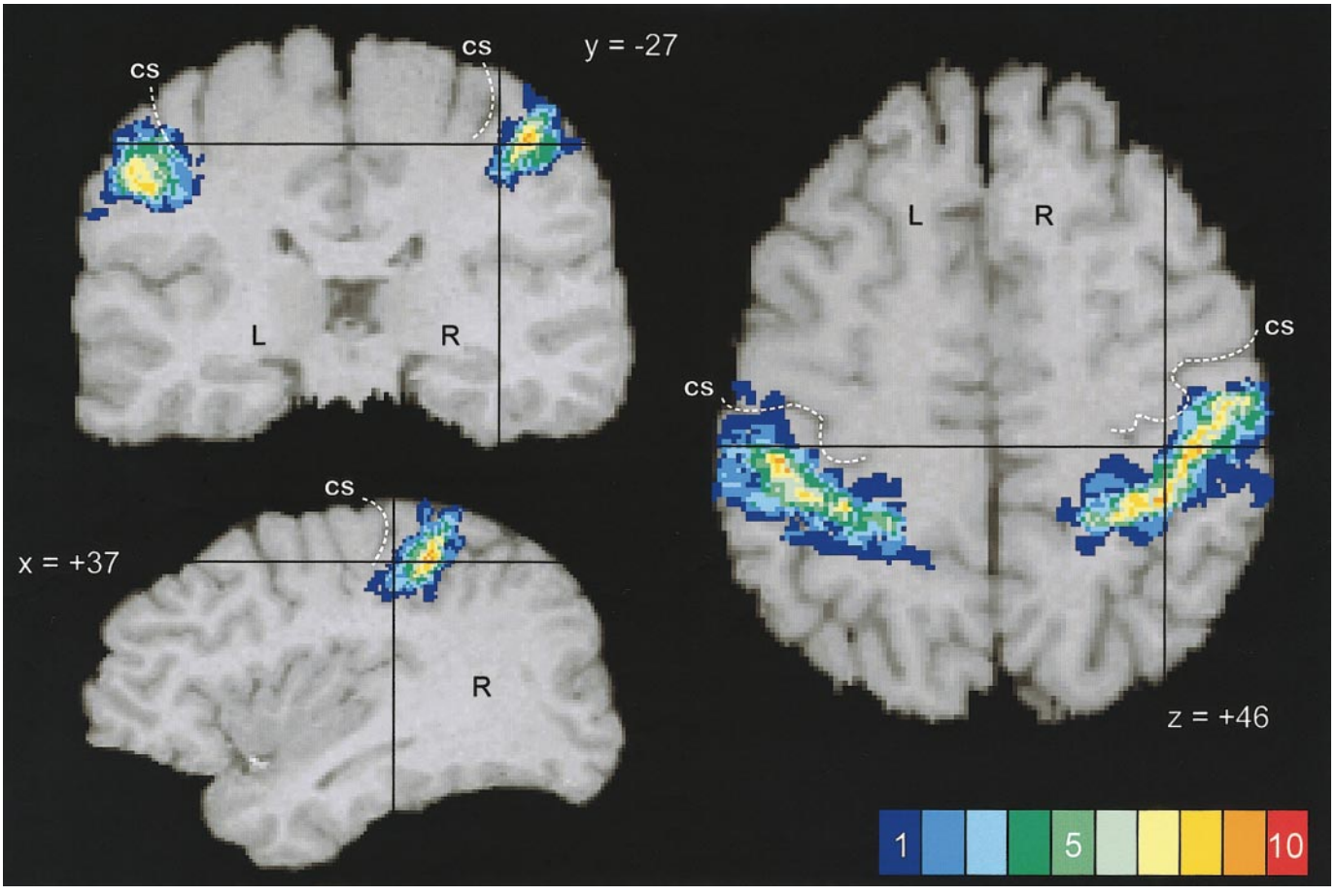

FIG. 7. Sagittal, coronal, and horizontal section through the reference brain (cf. cross reference markers) at Talairach coordinates $x = +37$ mm, $y = -27$ mm, and $z = +46$ mm. Population map of area 2 is superimposed. Representation of area 2 in n brains is color coded from dark blue ($n = 1$) to dark red ($n = 10$) (cf. color bar). L, left hemisphere; R, right hemisphere; cs, central sulcus.

hemisphere: $x_{medial} = +6$ mm, $x_{lateral} = +63$ mm, $y_{rostral} = +1$ mm, $y_{caudal} = -56$ mm, $z_{dorsal} = +71$ mm, $z_{ventral} = +20$ mm. Despite considerable interindividual variability, a clear focus (or representation in ≥50% of the brains) of area 2 is obvious in all three planes of sectioning. This focus lies in the caudal wall of the postcentral gyrus (or rostral wall of the postcentral sulcus). The volume of this 50% representation is: 2327 mm^3 (left), 2483 mm^3 (right), and 4810 mm^3 (left + right). The coordinates of the bounding box are for the left hemisphere: $x_{medial} = -16$ mm, $x_{lateral} = -54$ mm, $y_{rostral} = -19$ mm, $y_{caudal} = -46$ mm, $z_{dorsal} = +61$ mm, $z_{ventral} = +33$ mm. For the right hemisphere: $x_{medial} = +17$ mm, $x_{lateral} = +57$ mm, $y_{rostral} = -14$ mm, $y_{caudal} = -45$ mm, $z_{dorsal} = +58$ mm, $z_{ventral} = +38$ mm.

DISCUSSION

Validation of a Cytoarchitectonic Entity in the Caudal Wall of the Postcentral Gyrus

The cytoarchitecture of the postcentral gyrus has been studied several times over the last century (Brodmann, 1909; von Economo and Koskinas, 1925; Bailey and von Bonin, 1951; Sarkissov *et al.*, 1955). The areas delineated by the different investigators in the postcentral gyrus vary both in terms of number and topography. These discrepancies are partly due to interindividual biological variability but they are also the consequence of the subjectivity that in the past influenced all cytoarchitectonic parcellations (cf. Introduction). In order to exclude this latter confound, we have used an observer-independent technique to map the caudal wall of the postcentral gyrus. In our sample of 10 brains, we consistently found a cytoarchitectonically homogeneous entity in this region with a rostral border close to the caudal shoulder of the postcentral gyrus and a caudal border close to the fundus of the postcentral sulcus.

Unfortunately, Brodmann's publications (1903, 1908, 1909) are not very helpful in classifying this entity since they contain neither detailed verbal nor any pictorial descriptions of each area's cytoarchitectonic features. Instead, he only briefly comments on each area's topography. Caudal to area 1, Brodmann

TABLE 3A

Geometrical Pattern of the Postcentral Sulcus

	Right			Left			Total (right + left)		
	Present study	Ono *et al.* (1990)	Weighted means	Present study	Ono *et al.* (1990)	Weighted means	Present study	Ono *et al.* (1990)	Weighted means
Shape									
Continuous	70%	44%	**51.4%**	40%	48%	**45.7%**	55%	46%	**48.6%**
2 Segments	20%	40%	**34.3%**	40%	48%	**45.7%**	30%	44%	**40.0%**
3 Segments	10%	16%	**14.3%**	20%	4%	**8.6%**	15%	10%	**11.4%**
Superior End									
Extension to mesial side	20%	20%	**20.0%**	40%	40%	**40.0%**	30%	30%	**30.0%**
No extension to mesial side	80%	80%	**80.0%**	60%	60%	**60.0%**	70%	70%	**70.0%**
Inferior End									
Connection with SF	40%	68%	**60.0%**	30%	48%	**42.9%**	35%	58%	**51.4%**
No connection with SF	60%	32%	**40.0%**	70%	52%	**57.1%**	65%	42%	**48.6%**
Connection with IPS									
Yes	90%	64%	**71.4%**	90%	72%	**77.1%**	90%	68%	**74.3%**
No	10%	36%	**28.6%**	10%	28%	**22.9%**	10%	32%	**25.7%**

Note. The data by Ono *et al.* ($n = 25$) are listed next to our data ($n = 10$). Since we adapted the nomenclature of Ono *et al.*, weighted mean values of both studies ($n = 35$) are presented in bold in the third column. SF, Sylvian fissure; IPS, Intraparietal sulcus.

(1909) described an area 2 situated in the "caudal part of the gyrus centralis posterior or the anterior lip of the sulcus postcentralis." According to Brodmann, the posterior border of area 2 may sometimes be found caudal to the fundus of the postcentral sulcus. This is confirmed by our observations, but only in those regions where the postcentral sulcus is shallow (less than 0.5 cm deep, which is usually the case only close to its medial and lateral end). In contrast to Brodmann, von Economo and Koskinas (1925) meticulously described each area's cytoarchitectonic features and they also published photomicrographs. They delineated an area termed "P_D" in the caudal wall of the postcentral gyrus with cytoarchitectonic features (e.g., prominent pyramids in lower layer III which stand out in size compared to the cells in the other layers) that closely match our observations.

In the late 1950s Powell and Mountcastle (1959a) studied the cytoarchitecture of the postcentral gyrus of the rhesus monkey. Caudal to area 1 they described an area 2 whose cytoarchitectonic features are similar to the features we found in area 2 in humans. Powell and Mountcastle wrote: "An increase in the number of large pyramidal cells in the deeper parts of layer III (. . .) marks the transition between areas 1 and 2. In layer III the large pyramidal cells come to form quite a compact layer three to five cells thick (. . .). The superficial half of layer III becomes slightly less dense (. . .). Layers II and IV show little appreciable change (. . .)" (Powell and Mountcastle, 1959a, p. 115).

The entity that we delineated with our observer-independent technique is very similar to Brodmann's area 2, to area P_D as described by von Economo and Koskinas, and also to area 2 defined by Powell and Mountcastle in the rhesus monkey. We adopted Brodmann's nomenclature since it is more widely used and termed the entity "area 2."

TABLE 3B

Geometrical Pattern of the Intraparietal Sulcus

	Right			Left			Total (right + left)		
	Present study	Ono *et al.* (1990)	Weighted means	Present study	Ono *et al.* (1990)	Weighted means	Present study	Ono *et al.* (1990)	Weighted means
Shape									
Continuous	50%	28%	**34.3%**	70%	72%	**71.4%**	60%	50%	**52.9%**
2 Segments	40%	68%	**60.0%**	30%	28%	**28.6%**	35%	48%	**44.3%**
3 Segments	10%	4%	**5.7%**	0%	0%	**0%**	5%	2%	**2.8%**

Note. For further details, see legend of Table 3A.

Interindividual Variability in the Topography of Area 2

We found considerable topographical variability in the mediolateral extent of area 2. In some cases, the medial end of area 2 reaches to the midline whereas in other cases a gap of up to several millimeters was found between its medial end and the midline. Similar variability was detected in the topographical relation between the lateral end of area 2 and the Sylvian fissure. Quite unexpectedly, we did not find area 2 on the mesial cortical surface in the depth of the midline. As to this surprising result, conflicting data can be found in the "classical" cytoarchitectonic literature in humans: Brodmann (1909) and Sarkissov *et al.* (1955) found area 2 on the mesial surface whereas von Economo and Koskinas (1925) did not. In contrast, many studies in macaques (Vogt and Vogt, 1919; Powell and Mountcastle, 1959b; Burton and Jones, 1976; Pons *et al.*, 1985) described area 2 not only on the cortical convexity but also on the mesial surface. At variance with these latter results, a recent study by Lewis *et al.* (1999) did not find area 2 on the mesial surface of the macaque brain. However, Lewis *et al.* excluded all transition regions between area 2 and its cytoarchitectonic neighbors. This approach yielded a—what the authors termed—"lower bound estimate" of the extent of area 2. The resulting map showed an relatively small area surrounded by a cytoarchitectonic "no man's land"—a rather unsatisfying situation since two adjacent cortical areas should always have a common border. To sum up, the absence of area 2 from the mesial cortical surface in humans is in contrast with its extent in the macaque brain. To what extent this discrepancy reflects inter-observer differences in the structural delineation of area 2 or interspecies differences in its functional organization remains to be elucidated.

We also found topographical variability in the rostrocaudal extent of area 2. In some cases, the rostral end of area 2 reaches almost to the crown of the postcentral gyrus whereas in other cases it is hidden in the depth of the postcentral sulcus (cf. Figs. 2 and 5). Similar variability is obvious in the topographical relation between the caudal end of area 2 and the fundus of the postcentral sulcus. The postcentral sulcus is connected with the intraparietal sulcus in 90% (right and left hemisphere) in our sample and in 64% (right) and 72% (left) in Ono *et al.*'s (1990) sample (cf. Table 3A). We found that in these cases area 2 remains anchored to the postcentral sulcus and does not extend into the intraparietal sulcus. As to this result, conflicting data can be found in the "classical" cytoarchitectonic literature in humans: Brodmann (1909) and von Economo and Koskinas (1925) found an extension of area 2 or area P_D into the intraparietal sulcus whereas Sarkissov *et al.* (1955) did not. There is also a debate in literature whether or not area 2 can be found in the macaque's intraparietal sulcus. According to some authors (Vogt and Vogt, 1919; Peele, 1942; Powell and Mountcastle, 1959b; Burton and Jones, 1976; Vogt and Pandya, 1978) area 2 extends caudally to a varying degree into the intraparietal sulcus. However, in more recent studies (Shanks *et al.*, 1985; Pearson and Powell, 1985; Pons and Kaas, 1986; Burton and Fabri, 1995; Lewis *et al.*, 1999) area 2 was not found in this sulcus. What are the reasons for these differences? A key factor is the subjective nature of microstructural parcellation. Most of the authors cited above wrote that they had difficulties in unequivocally defining the caudal border of area 2. As a consequence, different investigators used different criteria and published maps which varied especially in the topography of the caudal border of area 2. In this study we attempted to solve this problem by delineating statistically significant borders with an observer-independent technique. Our results support those authors who did not find area 2 in the intraparietal sulcus. Interindividual biological variability is another reason for the discrepancies between the maps. Unfortunately, these cortical maps were published as sketches in a two-dimensional print format and a spatial reference system is not available which makes it difficult (especially in humans) to superimpose and compare these maps with each other. Considerable microanatomical variability, however, does exist. When histological volumes (with the volume representations of cortical areas) are spatially normalized in such a way that macroanatomical variability is minimized, each area's variability (as expressed in the population map) is almost exclusively microstructural in nature (cf. Geyer *et al.*, 2000). This remarkable degree of microstructural variability of area 2 is shown in the population map in Fig. 7.

In schematic drawings of the human cerebral cortex, the postcentral sulcus is typically depicted as a continuous and uninterrupted structure. The "classical" maps of Brodmann (1909), von Economo and Koskinas (1925), and many other investigators follow this simplification and depict both the postcentral sulcus and area 2 as a continuous mediolateral structure. No comments (neither verbally nor in pictorial format) are made on the course of area 2 when the postcentral sulcus is interrupted by a gyral bridge running between the postcentral gyrus and the posterior parietal cortex. In fact, our observations show that this case is by no means a rare variant. In our sample of 10 brains, the postcentral sulcus is interrupted by one (or even more) gyral bridges in 30% (right hemisphere) and 60% (left hemisphere). Ono *et al.* (1990) found in a sample of 25 brains interruptions of the postcentral sulcus in 56% in the right and 52% in the left hemisphere. As to the course of area 2 in such a case, one can imagine two possibilities: the area is either separated (just as the sulcus) into two segments by the cortical bridge or it is

not separated and crosses the bridge. To our knowledge, this topological problem has never been addressed in the published literature. We found in our sample that when the postcentral sulcus is interrupted by a gyral bridge, area 2 crosses this bridge and is not separated into two segments (cf. Fig. 6C and 6D, arrowhead).

Relationship between Structure and Function

The population map of area 2 may be used to interpret functional data on a more valid basis. The extent of area 2 can be defined as a VOI and matched with activation clusters in the postcentral region. For area 2, this has been done for the first time in a study by Bodegard *et al.* (2001, in press). Subjects had to perform different somatosensory tasks with their right hands: (i) passive tactile discrimination of ellipsoids and different brush stroke velocities, (ii) discrimination of edge length, curvature, and roughness, and (iii) active tactile discrimination of shapes. The authors demonstrated with PET and a subsequent cytoarchitectonic VOI analysis that area 2 was significantly more activated by shape and surface curvature changes than by texture, brush velocity, and edge length discrimination. In contrast, areas 3b and 1 were activated by all stimuli without any statistical differences. The preference of area 2 for the computation of shape and surface curvature changes is in accordance with findings in monkeys (Randolph and Semmes, 1974; Carlson, 1981; Iwamura *et al.*, 1983b), and supports the concept that also in humans area 2 is involved in a higher level of cortical somatosensory processing.

Therefore, a microstructural population map of area 2 as shown in this study is a promising way to learn more about its role in somatosensory processing in humans. When superimposed with statistical activation maps from PET or fMRI experiments or with equivalent current dipoles from MEG or EEG experiments, such a map should give a more valid answer to the question whether or not area 2 is being activated by a specific somatosensory task.

ACKNOWLEDGMENTS

The authors thank A. Schleicher, P. Weiss, and I. Toni for valuable advice and comments on the manuscript, H. Mohlberg for help with rendering the brains in 3-D, and U. Blohm and B. Machus for excellent technical assistance. Parts of this work have been supported by grants from the Deutsche Forschungsgemeinschaft (SFB 194/A6), the European Commission (BioMed 2 and BioTech programs), and the Human Brain Project (funded jointly by the National Institute of Mental Health, National Institute of Neurological Disorders and Stroke, National Institute on Drug Abuse, and the National Cancer Institute).

REFERENCES

Amunts, K., Malikovic, A., Mohlberg, H., Schormann, T., and Zilles, K. 2000. Brodmann's areas 17 and 18 brought into stereotaxic space—Where and how variable? *Neuroimage* **11:** 66–84.

Amunts, K., Schleicher, A., Bürgel, U., Mohlberg, H., Uylings, H. B. M., and Zilles, K. 1999. Broca's region revisited: Cytoarchitecture and intersubject variability. *J. Comp. Neurol.* **412:** 319–341.

Bailey, P., and von Bonin, G. 1951. *The Isocortex of Man.* University of Illinois Press, Urbana, IL.

Bodegard, A., Geyer, S., Naito, E., Zilles, K., and Roland, P. E. 2000. Somatosensory areas in man activated by moving stimuli: Cytoarchitectonic mapping and PET. *Neuroreport* **11:** 187–191.

Bodegard, A., Geyer, S., Grefkes, C., Zilles, K., and Roland, P. E. 2001. Hierarchical processing of tactile shape in the human brain. *Neuron,* in press.

Brodmann, K. 1903. Beiträge zur histologischen Lokalisation der Großhirnrinde. Erste Mitteilung: Die Regio Rolandica. *J. Psychol. Neurol.* **2:** 79–107.

Brodmann, K. 1908. Beiträge zur histologischen Lokalisation der Großhirnrinde. Sechste Mitteilung: Die Cortexgliederung des Menschen. *J. Psychol. Neurol.* **10:** 231–246.

Brodmann, K. 1909. *Vergleichende Lokalisationslehre der Großhirnrinde.* Barth, Leipzig.

Burton, H., and Fabri, M. 1995. Ipsilateral intracortical connections of physiologically defined cutaneous representations in areas 3b and 1 of macaque monkeys: Projections in the vicinity of the central sulcus. *J. Comp. Neurol.* **355:** 508–538.

Burton, H., and Jones, E. G. 1976. The posterior thalamic region and its cortical projection in new and old world monkeys. *J. Comp. Neurol.* **168:** 249–299.

Campbell, A. W. 1905. *Histological Studies on the Localization of Cerebral Function.* University Press, Cambridge.

Carlson, M. 1981. Characteristics of sensory deficits following lesions of Brodmann's areas 1 and 2 in the postcentral gyrus of Macacca mulatta. *Brain Res.* **204:** 424–430.

Costanzo, R. M., and Gardner, E. P. 1980. A quantitative analysis of responses of direction-sensitive neurons in somatosensory cortex of awake monkeys. *J. Neurophysiol.* **43:** 1319–1341.

Gardner, E. P., and Costanzo, R. M. 1980. Neuronal mechanisms underlying direction sensitivity of somatosensory cortical neurons in awake monkeys. *J. Neurophysiol.* **43:** 1342–1354.

Geyer, S., Ledberg, A., Schleicher, A., Kinomura, S., Schormann, T., Bürgel, U., Klingberg, T., Larsson, J., Zilles, K., and Roland, P. E. 1996. Two different areas within the primary motor cortex of man. *Nature* **382:** 805–807.

Geyer, S., Schleicher, A., and Zilles, K. 1999. Areas 3a, 3b, and 1 of human primary somatosensory cortex: 1. Microstructural organization and interindividual variability. *Neuroimage* **10:** 63–83.

Geyer, S., Schormann, T., Mohlberg, H., and Zilles, K. 2000. Areas 3a, 3b, and 1 of human primary somatosensory cortex: 2. Spatial normalization to standard anatomical space. *Neuroimage* **11:** 684–696.

Hari, R., Nagamine, T., Nishitani, N., Mikuni, N., Sato, T., Tarkiainen, A., and Shibasaki, H. 1996. Time-varying activation of different cytoarchitectonic areas of the human SI cortex after tibial nerve stimulation. *Neuroimage* **4:** 111–118.

Hyvärinen, J., and Poranen, A. 1978. Receptive field integration and submodality convergence in the hand area of the post-central gyrus of the alert monkey. *J. Physiol. London* **283:** 539–556.

Iwamura, Y., Tanaka, M., Sakamoto, M., and Hikosaka, O. 1983b. Converging patterns of finger representation and complex re-

sponse properties of neurons in area 1 of the first somatosensory cortex of the conscious monkey. *Exp. Brain Res.* **51:** 327–337.

Iwamura, Y., Tanaka, M., Sakamoto, M., and Hikosaka, O. 1983a. Functional subdivisions representing different finger regions in area 3 of the first somatosensory cortex of the conscious monkey. *Exp. Brain Res.* **51:** 315–326.

Kaas, J. H. 1993. The functional organization of somatosensory cortex in primates. *Ann. Anatomy* **175:** 509–518.

Kaas, J. H. 1997. Somatosensory cortex. In *Encyclopedia of Neuroscience (CD-ROM Edition)* (G. Adelman and B. H. Smith, Eds.), Elsevier, Amsterdam.

Lewis, J. W., Burton, H., and Van Essen, D. C. 1999. Anatomical evidence for the posterior boundary of area 2 in the macaque monkey. *Somatosens. Motor Res.* **16:** 382–390.

Mahalanobis, P. C., Majumda, D. N., and Rao, C. R. 1949. Anthropometric survey of the united provinces. A statistical study. *Sankhya* **9:** 89–324.

Merker, B. 1983. Silver staining of cell bodies by means of physical development. *J. Neurosci. Methods* **9:** 235–241.

Ono, M., Kubik, S., and Abernathey, C. D. 1990. *Atlas of the Cerebral Sulci.* Thieme, Stuttgart.

Pearson, R. C. A., and Powell, T. P. S. 1985. The projection of the primary somatic sensory cortex upon area 5 in the monkey. *Brain Res. Rev.* **9:** 89–107.

Peele, T. L. 1942. Cytoarchitecture of individual parietal areas in the monkey (Macaca mulatta) and the distribution of the efferent fibers. *J. Comp. Neurol.* **77:** 693–738.

Pons, T. P., Garraghty, P. E., Cusick, C. G., and Kaas, J. H. 1985. The somatotopic organization of area 2 in macaque monkeys. *J. Comp. Neurol.* **241:** 445–466.

Pons, T. P., and Kaas, J. H. 1986. Corticocortical connections of area 2 of somatosensory cortex in macaque monkeys: A correlative anatomical and electrophysiological study. *J. Comp. Neurol.* **248:** 313–335.

Powell, T. P. S., and Mountcastle, V. B. 1959b. Some aspects of the functional organization of the cortex of the postcentral gyrus of the monkey: A correlation of findings obtained in a single unit analysis with cytoarchitecture. *Bull. Johns Hopk. Hosp.* **105:** 133–162.

Powell, T. P. S., and Mountcastle, V. B. 1959a. The cytoarchitecture of the postcentral gyrus of the monkey macaca mulatta. *Bull. Johns Hopk. Hosp.* **105:** 108–131.

Rademacher, J., Caviness, V. S., Steinmetz, H., and Galaburda, A. M. 1993. Topographical variation of the human primary cortices: Implications for neuroimaging, brain mapping, and neurobiology. *Cereb. Cortex* **3:** 313–329.

Rajkowska, G., and Goldman-Rakic, P. S. 1995. Cytoarchitectonic definition of prefrontal areas in the normal human cortex: II. Variability in locations of areas 9 and 46 and relationship to the Talairach coordinate system. *Cereb. Cortex* **5:** 323–337.

Randolph, M., and Semmes, J. 1974. Behavioral consequences of selective subtotal ablations in the postcentral gyrus of *macaca mulatta*. *Brain Res.* **70:** 55–70.

Roland, P. E., Geyer, S., Amunts, K., Schormann, T., Schleicher, A., Malikovic, A., and Zilles, K. 1997. Cytoarchitectural maps of the human brain in standard anatomical space. *Hum. Brain Mapp.* **5:** 222–227.

Roland, P. E., Graufelds, C. J., Wåhlin, J., Ingelman, L., Andersson, M., Ledberg, A., Pedersen, J., Åkerman, S., Dabringhaus, A., and Zilles, K. 1994. Human brain atlas: For high-resolution functional and anatomical mapping. *Hum. Brain Mapp.* **1:** 173–184.

Roland, P. E., and Zilles, K. 1994. Brain atlases—A new research tool. *Trends Neurosci.* **17:** 458–467.

Roland, P. E., and Zilles, K. 1996. Functions and structures of the motor cortices in humans. *Curr. Opin. Neurobiol.* **6:** 773–781.

Ruiz, S., Crespo, P., and Romo, R. 1995. Representation of moving tactile stimuli in the somatic sensory cortex of awake monkeys. *J. Neurophysiol.* **73:** 525–537.

Sarkissov, S. A., Filimonoff, I. N., Kononowa, E. P., Preobraschenskaja, I. S., and Kukuew, L. A. 1955. *Atlas of the Cytoarchitectonics of the Human Cerebral Cortex.* Medgiz, Moscow.

Schleicher, A., Amunts, K., Geyer, S., Morosan, P., and Zilles, K. 1999. Observer-independent method for microstructural parcellation of cerebral cortex: A quantitative approach to cytoarchitectonics. *Neuroimage* **9:** 165–177.

Schleicher, A., Amunts, K., Geyer, S., Schormann, T., Kowalski, T., Palomero-Gallagher, N., and Zilles, K. 2000. A stereological approach to human cortical architecture: Identification and delineation of cortical areas. *J. Chem. Neuroanat.* **20:** 31–47.

Schleicher, A., and Zilles, K. 1990. A quantitative approach to cytoarchitectonics: Analysis of structural inhomogeneities in nervous tissue using an image analyser. *J. Microsc.* **157:** 367–381.

Schormann, T. 1998. Method for computing and displaying 2D- and 3D-spatial differences of structures. International Patent PCT/EP99/04442.

Schormann, T., Dabringhaus, A., and Zilles, K. 1995. Statistics of deformations in histology and application to improved alignment with MRI. *IEEE Trans. Med. Imaging* **14:** 25–35.

Schormann, T., Dabringhaus, A., and Zilles, K. 1997b. Extension of the principal-axes theory for the determination of affine transformations. In *Mustererkennung 1997 (19. DAGM-Symposium, Braunschweig, 15.–17. September 1997)* (E. Paulus and F. M. Wahl, Eds.), pp. 384–391. Springer, Berlin.

Schormann, T., Henn, S., Bürgel, U., Engler, K., and Zilles, K. 1997a. A new technique for 3-D nonlinear deformation: Application to studies of the variability of brain structures. *Neuroimage* **5:** S418.

Schormann, T., Henn, S., and Zilles, K. 1996. A new approach to fast elastic alignment with application to human brains. *Lect. Notes Comput. Sci.* **1131:** 437–442.

Schormann, T., von Matthey, M., Dabringhaus, A., and Zilles, K. 1993. Alignment of 3-D brain data sets originating from MR and histology. *Bioimaging* **1:** 119–128.

Schormann, T., and Zilles, K. 1997. Limitations of the principal-axes theory. *IEEE Trans. Med. Imaging* **16:** 942–947.

Schormann, T., and Zilles, K. 1998. Three-dimensional linear and nonlinear transformations: An integration of light microscopical and MRI data. *Hum. Brain Mapp.* **6:** 339–347.

Shanks, M. F., Pearson, R. C. A., and Powell, T. P. S. 1985. The ipsilateral cortico-cortical connexions between the cytoarchiteconic subdivisions of the primary somatic sensory cortex in the monkey. *Brain Res. Rev.* **9:** 67–88.

Vogt, B. A., and Pandya, D. N. 1978. Cortico-cortical connections of somatic sensory cortex (areas 3, 1 and 2) in the rhesus monkey. *J. Comp. Neurol.* **177:** 179–191.

Vogt, C., and Vogt, O. 1919. Allgemeinere Ergebnisse unserer Hirnforschung. *J. Psychol. Neurol.* **25:** 279–461.

von Economo, K., and Koskinas, G. 1925. *Die Cytoarchitektonik der Hirnrinde des erwachsenen Menschen.* Springer, Wien.

Warren, S., Hämäläinen, H. A., and Gardner, E. P. 1986. Objective classification of motion- and direction-sensitive neurons in primary somatosensory cortex of awake monkeys. *J. Neurophysiol.* **56:** 598–622.

White, L. E., Andrews, T. J., Hulette, C., Richards, A., Groelle, M., Paydarfar, J., and Purves, D. 1997. Structure of the human sensorimotor system. I: Morphology and cytoarchitecture of the central sulcus. *Cereb. Cortex* **7:** 18–30.